rf resistance and inductance of massively parallel single walled carbon nanotubes: Direct, broadband measurements and near perfect 50 Ω impedance matching

Chris Rutherglen, Dheeraj Jain, and Peter Burke[a]
Department of Electrical Engineering and Computer Science, University of California, Irvine, California 92697, USA

(Received 14 June 2008; accepted 13 July 2008; published online 28 August 2008)

We report using dielectrophoresis to accumulate hundred to thousands of solubilized single walled carbon nanotubes in parallel to achieve impedance values very close to 50 Ω. This allows us to clearly measure the real (resistive) and imaginary (inductive) impedance over a broad frequency range. We find a negligible to mild frequency dependent resistance for the devices and an imaginary impedance that is significantly smaller then the resistance over the range of dc to 20 GHz. This clearly and unambiguously demonstrates that kinetic inductance is not the major issue facing nanotube array interconnects, when compared to the real impedance (the resistance). © *2008 American Institute of Physics*. [DOI: 10.1063/1.2970031]

The potential use of single walled carbon nanotubes (SWNTs) as high frequency on-chip interconnects is motivated by their high intrinsic conductivity, comparable to or larger than Cu.[1,2] However, an open issue is the roll of the kinetic inductance, which is predicted to be much larger than the magnetic inductance.[3,4] Complicating this analysis is the fact that, for a single nanotube, the resistance (as opposed to the resistivity) is very high, of order 10 kΩ/μm.[1,5] This makes the use of individual SWNTs as interconnects unlikely in conventional electronics, and requires parallel nanotubes for realistic applications.

Few measurements of the radio-frequency (rf) impedance of individual metallic nanotubes have been performed,[6,7] in large part because of the difficulty in calibrating and measuring systems with impedance much larger than 50 Ω. These results have yielded measurements consistent with predictions.[3] In contrast, there are several measurements of parallel arrays of carbon nanotubes (CNTs) at rf. Pesetski *et al.*[8] measured SWNTs arrays of ~10 tubes, with a dc resistance of ~ 1 k$\Omega = 10\times$ larger than 50 Ω. Plombon *et al.*[7] also measured bundles with a dc resistance of 750 $\Omega \sim 10 \times 50$ Ω. Both used a transmission geometry. Plombon *et al.* found evidence for kinetic inductance. Le Louarn *et al.* fabricated nanotube FETs and demonstrated the highest cutoff frequency to date.[9]

Here we report using solubilized SWNTs and dielectrophoresis (DEP) to accumulate hundreds to thousands of SWNTs in parallel to achieve resistances very close to 50 Ω for frequencies from dc to 20 GHz. Inductances of the devices were measured to be much smaller than the resistance. These measurements are different and significant over prior measurements in that (1) an almost perfect 50 Ω impedance match is obtained, a major milestone for CNT technology that as recent as a few years ago, was a mere idea (prior metallic SWNT arrays were at least an order of magnitude larger than 50 Ω); (2) our measurements provide *direct* measurements of the *physically meaningful* impedance of arrays of SWNTs (rather than the concentrating on the S parameters) including both the real *and* the imaginary impedance; (3) because of point 2, our measurements for the first time clearly and unambiguously demonstrate that kinetic inductance is not the major issue facing nanotube array interconnects. This is discussed in the conclusions.

Figure 1 shows the layout for our measurements. Using electron beam lithography, electrodes with a pair of 3 μm gap spacing were patterned and evaporated with Ti/Au (5 nm/50 nm) on high resistivity Si wafers (>8000 Ω cm) with a 500 nm thermal oxide layer. Coplanar waveguide electrode geometries were patterned with photolithography and evaporated with 25 nm Ti/250 nm Au to form a dual waveguide/electrode structure with a pair of 3 μm long (L) electrode gaps and with actual widths (W) of 100 μm. After accumulation of aligned SWNTs within the gap by DEP, as described further in this letter, contact electrodes were patterned using e-beam lithography and evaporated with 70 nm of Pd producing a new electrode gap of 1 μm, which is seen in Fig. 1. The devices were rf-electrically contacted using a commercially available probe. S_{11} measurements were taken using an Agilent 8720ES network analyzer with a frequency span of 50 MHz–20 GHz.

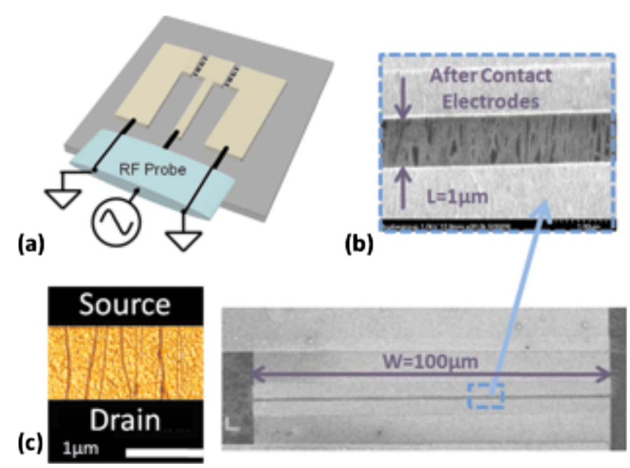

FIG. 1. (Color online) (a) Diagram of the rf probing and dual coplanar waveguide/electrode structure. (b) SEM images of solubilized SWNT accumulated by DEP within the gap of width, $W=100$ μm, and length, $L=1$ μm. (c) AFM image of a low-density region of CNTs with measured tube/bundle diameters of 2–8 nm.

[a]Electronic mail: pburke@uci.edu.

0003-6951/2008/93(8)/083119/3/$23.00

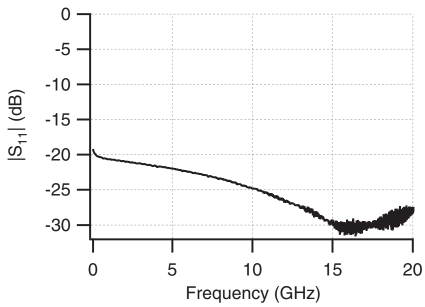

FIG. 2. S_{11} magnitude for a typical device with an electrode-gap width of 100 μm.

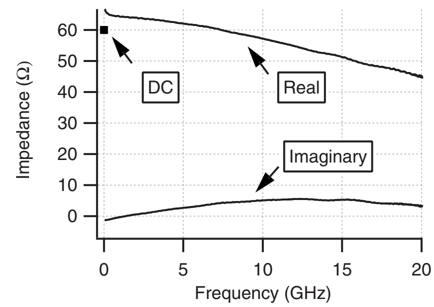

FIG. 3. Calibrated impedance traces of SWNTs on the 100 μm electrode width devices.

Commercially available purified SWNT manufactured by arc method and with an OD 1.2–1.4 nm were used to make the devices. These SWNTs were dispersed by sonicating for 20 min in 1% (w/v) sodium cholate aqueous solution and centrifuged at 16 000 rpm for 3 h to remove large debris and clumps of nanotubes. Using a glass micropipette with a tip diameter of ~20 μm, the supernatant was placed on the electrodes and DEP was used to accumulate the solubilized SWNTs within the electrode gap.[10] This was accomplished using a 4–5 V_{pp}, 25 MHz sine wave voltage signal applied to the electrodes for 2 min. The residue of the solute precipitate remaining after evaporation was gently washed away with dH_2O.

Subsequent scanning electron microscope (SEM) imaging of the SWNTs show large accumulations of aligned SWNTs within the electrode gaps, as shown in Fig. 1(b). The bulk of the accumulated nanotubes were found to have lengths of ~3–5 μm length and consequently fit well with the 3 μm gap length used. Based on these images we estimate the tube density to be 10 nanotubes/μm. We found the dc resistance changed 16%, 42–50 Ω, when the gate voltage varied between V_g=−35 V and V_g=+35 V, indicating that the majority of the SWNTs deposited are metallic. This result is consistent with prior work showing that semiconducting nanotubes are expelled from the high electric fields region within the electrode gap due to negative DEP for frequencies greater than the crossover frequency of roughly 10 MHz. In contrast, the metallic nanotubes have been shown to experience positive DEP well above 30 MHz since the crossover frequency for them is much higher relative to the semiconducting type.[11] All devices for this paper were accumulated by DEP with a frequency of 25 MHz.

The SEM images taken of the accumulated nanotubes within the electrode gap showed densities in excess of 10 CNTs/μm in most cases [see Fig. 1(b)]. Further imagery characterization was taken using an atomic force microscope (AFM) after annealing the devices 20 min at 200 C in argon to remove any surface residue. Individual SWNTs and small bundles were observed with diameters ranging from 1.5–8 nm (see Fig. 2, inset). Both SEM and AFM images confirm that most of the CNTs completely span the electrode gap.

Calibration up to the rf-probe electrodes were obtained using standard one-port, S_{11}, open/short/load calibration in addition to further calibration, as discussed in Ref. 12. A commercially available microwave probe (suitable for calibration with a commercially available open/ short/load calibration standard) allowed for transition from coax to lithographically fabricated on chip electrodes. Measurements were performed at a power level of −15 dBm. A microwave network analyzer is used to measure the calibrated (complex) reflection coefficient $S_{11}(\omega) \equiv V_{\text{reflected}}/V_{\text{incident}}$, where V_{incident} is the amplitude of the incident microwave signal on the coax, and similarly for $V_{\text{reflected}}$. This is related to the load impedance $Z(\omega)$ by the usual reflection formula,

$$S_{11} = [Z(\omega) - 50\ \Omega]/[Z(\omega) + 50\ \Omega]. \tag{1}$$

In our experiments, an extra length (~1 mm) of on-chip coplanar waveguide transmission line was added to offset the nanotube location from the probes, so that the probes would not interfere with the aliquot during the DEP deposition. This required an additional phase and magnitude correction to the measured S_{11}, described in Ref. 12. The uncertainty in the phase is discussed in detail below. The magnitude correction was less than 2 dB.

Before discussing the impedance, we first discuss the magnitude of the measured value of S_{11}. While the impedance is sensitive to the calibrations (see below), the measured magnitude of S_{11} is much less sensitive to calibration uncertainties. In Fig. 2, we plot the value of S_{11} versus frequency for a typical device measured in this work. The measured value of S_{11} is between −20 and −30 dB over the entire band. In microwave engineering, this is considered an outstanding impedance match, since even connectors can have worse reflection coefficients. A central result of this paper, this clearly represents close to ideal broadband impedance matching of a nanotechnology based device to a 50 Ω rf system.

We now turn to the real and imaginary impedance for our devices, plotted in Fig. 3. We begin our discussion of the real impedance by considering the device studied in Fig. 3(a), which has a width of 100 μm and a gap of 1 μm. Real impedance values of ~50 Ω and as low as 2 Ω for very high density nanotubes accumulations, were obtained for these devices. Furthermore, the impedance was approximately halved when the electrode gap length was reduced from 1.0 to 0.6 μm indicating that the contact resistance is significantly less than the length-dependent resistance. The real impedance is approximately independent of frequency and equal to its dc value over the entire frequency range studied.

In order to predict the dc resistance, we need to know the contact resistance per nanotube R_C, the number of nanotubes N, and the resistance per length of each nanotube R, and the length of the gap L. The total resistance will then be given by

$$R_{\text{dc}} = (R_C + R^* L)/N. \tag{2}$$

If the nanotubes are shorter than the gap, and if the nanotubes are not perfectly aligned then there will be additional resistance[13] so that (2) corresponds to an estimate of the lower limit of the dc resistance. A rough estimate for the number of SWNTs based on the SEM image is 10 CNTs/μm of length, for a total of 2000 SWNTs for a $W_{\mathrm{effective}}=200$ μm gap width. Considering that the contact resistance is greater than 6.5 kΩ and the resistance per unit length is approximately 10 kΩ/μm,[1,5] we arrive at a predicted dc resistance of 8 Ω. Furthermore, since the number of nanotubes is not well known, this is reasonably consistent with the measured value of 65 Ω for the device in Fig. 3(b).

We now turn to a discussion of the imaginary impedance. In our experiments, within our calibration uncertainty, the imaginary impedance was much less than the real impedance all the way to 20 GHz. This clearly and unambiguously demonstrates that kinetic inductance is not the major issue facing nanotube array interconnects, when compared to the real impedance (the resistance). We first discuss the predicted kinetic inductance, and then its interpretation.

The predicted kinetic inductance for a SWNT is 4 nH/μm.[3] The total inductance should be the kinetic inductance per length L_{ind} times the length L divided by the number of nanotubes N, i.e.,

$$L_{\mathrm{total}} = L_{\mathrm{ind}}{}^{*}L/N. \tag{3}$$

This leads to an estimate of 8 pH, which would give rise to an inductive impedance, L_{total}, of 0.5 Ω at 10 GHz. This prediction is in complete agreement with our measurements, which finds a value of 0 ± 10 Ω at 10 GHz for the imaginary impedance. Thus, our measurements are completely consistent with the measured value.

A separate issue is that of the capacitance. In our measurements, only a common mode voltage is excited (each nanotube is electrically contacted), so we do not expect any differential voltage between any two nanotubes.[14] Thus, nanotube-to-nanotube capacitance is not probed by our measurements. The intrinsic (quantum) capacitance is sufficiently small that it is not expected to be measureable in our experiments.

We now discuss the implications of our work for potential use of nanotubes as interconnects. The primary conclusion of our experimental work is that the real impedance dominates over the inductive impedance for massively parallel SWCNT array from DC to over 20 GHz. This makes complete sense according to the following simple argument: The predicted inductance per unit length is 4 nH/μm.[3] The measured resistance per unit length is 10 kΩ/μm.[1,5] Thus, the inductance impedance, which rises linearly with frequency as $i\omega L$, is only comparable to the resistive impedance at 200 GHz, much higher than the frequency range measured herein.

In our prior work on individual nanotubes,[6] because of the high impedance, we were unable to carefully measure the imaginary impedance. Achieving near perfect 50 Ω impedance matching of massively parallel SWCNT represents an important step forward because in this work it has allowed us, with only moderate effort on the calibration, to clearly measure the real and imaginary impedance.

The implication for interconnects is that the inductive impedance is not significant over this frequency range compared to the resistive impedance, and that the resistive impedance deserves the first priority when comparing SWNTs as interconnects to copper. With this clear experimental demonstration we aim to dispel the notion, once and for all, that kinetic inductance prohibits the use of nanotubes as interconnects. In fact, the resistive impedance is much larger and must be addressed first. That said, the resistivity of a nanotube is lower than copper, so that the practical use of interconnects is possible and potentially advantageous over Cu.

Our measurements very clearly indicate that an equivalent circuit model of a pure resistor is approximately appropriate to describe both the real and the imaginary impedance of massively parallel SWNT arrays from dc to 20 GHz. While other authors have provided much more elaborate circuit models based on combinations of multiple (>10) discrete components (resistors, inductors, and capacitors), we do not believe in our case our calibrations or data are accurate enough to meaningfully invoke any such model. Future work with improved calibration may be able to support such a model for massively parallel arrays. In fact, the complete circuit model should not consist of discrete elements, but rather distributed elements at the contacts, and along the nanotube.[3] A systematic comparison of when discrete versus simulated elements are appropriate, and to what degree of accuracy, has yet to be performed (although work is in progress along those lines[3,4]), and is left as a project for future research.

The authors would like to thank the help of M. Strano for useful discussion. This work was supported by the Office of Naval Research, the National Science Foundation, and a gift from Northrop Grumman.

[1]S. Li, Z. Yu, C. Rutherglen, and P. J. Burke, Nano Lett. **4**, 2003 (2004).
[2]P. J. Burke, Z. Yu, and C. Rutherglen, in *Nanowires and Nanotubes*, edited by P. J. Burke (World Scientific, Singapore, 2007); M. P. Anantram and F. Leonard, Rep. Prog. Phys. **69**, 507 (2006).
[3]P. J. Burke, IEEE Trans. Nanotechnol. **2**, 55 (2003).
[4]S. Salahuddin, M. Lundstrom, and S. Datta, IEEE Trans. Electron Devices **52**, 1734 (2005); A. Naeemi, R. Sarvari, and J. D. Meindl, IEEE Electron Device Lett. **26**, 84 (2005); A. Naeemi and J. D. Meindl, *ibid.* **26**, 476 (2005); A. Naeemi and J. D. Meindl, *ibid.* **26**, 544 (2005); A. Nieuwoudt and Y. Massoud, *ibid.* **28**, 305 (2007); A. Nieuwoudt and Y. Massoud, IEEE Trans. Electron Devices **53**, 2460 (2006); A. Nieuwoudt and Y. Massoud, IEEE Trans. Nanotechnol. **l5**, 758 (2006).
[5]M. S. Purewal, B. H. Hong, A. Ravi, B. Chandra, J. Hone, and P. Kim, Phys. Rev. Lett. **98**, 186808 (2007).
[6]Z. Yu and P. J. Burke, Nano Lett. **5**, 1403 (2005).
[7]J. J. Plombon, K. P. O'Brien, F. Gstrein, V. M. Dubin, and Y. Jiao, Appl. Phys. Lett. **90**, 063106 (2007).
[8]A. A. Pesetski, J. E. Baumgardner, E. Folk, J. X. Przybysz, J. D. Adam, and H. Zhang, Appl. Phys. Lett. **88**, 113103 (2006).
[9]A. Le Louarn, F. Kapche, J.-M. Bethoux, H. Happy, G. Dambrine, V. Derycke, P. Chenevier, N. Izard, F. Goffman, and J.-P. Bourgoin, Appl. Phys. Lett. **90**, 233108 (2007).
[10]K. Yamamoto, S. Akita, and Y. Nakayama, Jpn. J. Appl. Phys., Part 2 **35**, L917 (1996).
[11]Y. Kim, S. Hong, S. Jung, M. S. Strano, J. Choi, and S. Baik, J. Phys. Chem. B **110**, 1541 (2006); S. Baik, M. Usrey, L. Rotkina, and M. Strano, J. Phys. Chem. B **108**, 15560 (2004); R. Krupke, F. Hennrich, M. M. Kappes, and H. V. Lohneysen, Nano Lett. **4**, 1395 (2004); R. Krupke, F. Hennrich, H. B. Weber, M. M. Kappes, and H. v. Löhneysen, Nano Lett. **3**, 1019 (2003).
[12]See EPAPS Document No. E-APPLAB-93-103832 for the rf calibration method used to remove resitive loss and phase lag associated with the coplanar wavegude. For more information on EPAPS see http://www.aip.org/pubservs/epaps.html.
[13]N. Pimparkar, J. Guo, and M. A. Alam, IEEE Trans. Electron Devices **54**, 637 (2007).
[14]Q. Cao, M. G. Xia, C. Kocabas, M. Shim, J. A. Rogers, and S. V. Rotkin, Appl. Phys. Lett. **90**, 023516 (2007).